Journal of Education for Pure Science
Vol.16, No. 02 (2026)
DOI: https://doi.org/10.32792/jeps.v16i2.889
Website: jceps.utq.edu.iq Email: jceps@eps.utq.edu.iq

Mamadu-Njoseh Polynomial-Based Projected Heun Method for Solving Initial Value Problems

Ebimene James Mamadu[*,1], Jude Chukwuyem Nwankwo[2], Inonoje S.O.Emmanuel[3], Otaide I. Jackson[4], Ebikonbo-Owei A. Mamadu[1], Irerhievwie Oghenetega Stephen[5], Henrietta Ify Ojarikre[1], Ignatius Nkonyeasua Njoseh[1]

[1]Department of Mathematics, Delta State University, Abraka, Nigeria
[2] Department of Mathematics, University of Delta, Agbor, Nigeria
[3] Department of Mathematics, Southern Delta University, Ozoro, Nigeria
[4] Federal University of Petroleum Resources, Effurun, Delta State, Nigeria
[5] Department of General Studies, Petroleum Training Institute, Effurun, Delta State, Nigeria

[*] Corresponding email: emamadu@delsu.edu.ng

Received 25 / 01 /2026, Accepted 22 / 05 /2026, Published 01 / 06 /2026

Abstract:

This paper introduces a Projected Heun Scheme (PHS) based on Mamadu-Njoseh polynomials for solving linear and nonlinear Initial Value Problems (IVPs). The scheme preserves the second-order convergence of the classical Heun method but achieves faster convergence and improved accuracy, particularly for nonlinear and oscillatory systems. A detailed stability analysis confirms its wider stability region, making it a robust and efficient tool for high-precision numerical solution of IVPs in computational science and applied mathematics.

Keywords: Heun's method; Initial value problems; Mamadu-Njoseh polynomials; Projection; Stability; Differential equations.

1-Introduction Section

The study of Initial Value Problems (IVPs) in the form of

$$\frac{dy}{dt} = f(t,y), y(t_0) = y_0,\ t \in [t_0, T], \tag{1.1}$$

It is fundamental to computer science and applied mathematics. Modeling time-dependent phenomena in physics, engineering, biology, and finance, including systems like electrical circuits, population dynamics, mechanical oscillators, chemical kinetics, and fluid flows, naturally presents these kinds of issues [1], [2]. Only in certain situations, usually linear or separable problems, do analytical solutions for IVPs exist; they are rarely accessible for stiff or nonlinear systems. As a result, numerical techniques are now essential tools for estimating solutions with achievable precision [3].

Among classical numerical methods, Euler's method offers the simplest approximation by assuming the slope of the solution stays constant over each step. However, this method has a first-order accuracy and can lead to large errors over long intervals or stiff systems. To address these issues, higher-order methods, like the Runge-Kutta family, are often used. In particular, Heun's method, also known as the improved Euler method or the explicit trapezoidal method, offers a second-order accurate predictor-corrector scheme that averages the slope at both the beginning and the end of each step [4,5].

Mathematically, for a step size h, Heun's method approximates the solution of (1.1) at $t_{n+1} = t_n + h$ as

$$y_{n+1}^{(p)} = y_n + f(t_n, y_n), \quad \text{(Predictor)} \tag{1.2}$$

$$y_{n+1} = y_n + \frac{h}{2}\left(f(t_n, y_n) + f(t_{n+1}, y_{n+1}^{(p)})\right), \quad \text{(Corrector)} \tag{1.3}$$

where $y_{n+1}^{(p)}$ is the Euler predictor. While this method improves accuracy, error accumulation and instability can still occur when solving long-time dynamics or nonlinear systems [6,7].

The Mamadu–Njoseh (MN) polynomials are a novel orthogonal polynomial defined on $[-1,1]$ with a weight function $w(t) = 1 + t^2$. Orthogonal polynomial-based projection methods have been known for enhancing or further improving the numerical accuracy and stability of many numerical schemes [2,5]. One can minimize the residual error and maintain desirable smoothness properties by projecting the numerical solution onto a basis of orthogonal polynomials [8-14].

The Mamadu-Njoseh polynomials $\{\varphi_n(x)\}_{n=0}^{\infty}$ satisfy the orthogonality condition

$$\int_{-1}^{1} \varphi_n(x)\varphi_m(x)w(x)dx = 0, n \neq m, \tag{1.4}$$

and can be normalized to improve numerical performance and stability [15,16]. These polynomials offer a strong projection foundation that lowers global errors by enabling approximate solutions to meet a weighted residual orthogonality constraint.

In this work, we propose a Projected Heun Scheme (PHS) using Mamadu–Njoseh Polynomials [14], which combines the projection capabilities of MN polynomials with the second-order precision of Heun's approach. Even for long-term integration or extremely nonlinear systems, this projection guarantees reduced residual error, smooth solution profiles, and enhanced numerical stability. The proposed approach offers a reliable, effective, and extremely precise tool for resolving IVPs in applied mathematics, physics, engineering, and other computational domains by bridging the gap between traditional numerical schemes and contemporary polynomial-based projections. The method is a viable option for large-scale simulations and real-world applications since it works especially well when traditional approaches are unable to control error propagation or call for adaptive step refinement [17].

2- Preliminaries

Let

$$\frac{dy}{dt} = f\big(t, y(t)\big), y(t_0) = y_0, t \in [t_o, T], \tag{2.1}$$

with $f: [t_0, T] \times \mathbb{R}^d \longrightarrow \mathbb{R}^d$, where $\mathbb{R}^d$ denotes d-dimensional real space.

We consider the following assumptions.

A1. f is continuous at t and Lipschitz at $y \Longrightarrow \exists\, L > 0$ such that

$$\|f(t, y_1) - f(t, y_2)\| \leq l\|y_1 - y_2\| \; \forall \; t \in [t_0, T], \forall \; y_1, y_2 \in \mathbb{R}^d.$$

A2. $y \in C^3([t_0, T];\ \mathbb{R}^d) \Longrightarrow$ the exact solution $y(t)$ is sufficiently smooth.

A3. $\{\varphi_j(\xi)\}_{j=0}^{\infty}$ are Mamadu-Njoseh polynomials defined on $\xi \in [-1,1]$ with weight function $w(\xi) = 1 + \xi^2$, and Π_m denote the original projection into $\Psi_m := span\,\{\varphi_0, \ldots, \varphi_m\}$ with respect to the

weighted inner product

$$< u, v >_w = \int_{-1}^{1} u(\xi)v(\xi)w(\xi)d\xi. \quad (2.2)$$

A4. Define the projection error as

$$\epsilon_M(t) = \|y(t) - \Pi_m y(t)\|_{L^\infty(\Omega)},$$

where Ω denotes the mapped domain for the projection evaluation. We also assume $\epsilon_M(t) \longrightarrow 0$ as $M \longrightarrow \infty$, and $\epsilon_M \coloneqq \sup_{t\in[t_0,T]} \epsilon_M(t)$.

A5. When we approximate inner products and integrals numerically (quadrature), there is quadrature error Q_{quad} that will be accounted for in the final bounds.

A6. The time interval $[t_0, T]$ is partitioned into N_t equal uniform steps $t_n = t_0 + nh, n = 0, \dots, N$, with $h = \frac{(T-t_0)}{N_t}$.

A7. $\|\cdot\|$ denotes the Eucludean norm for vectors; where needed we use the weighted L^2_w norm on $[-1,1]$, that is, $\|u\|^2_{L^2_w} =< u, u >_w$.

3- Projected-Heun Scheme

Let Π_m denote orthogonal projection into the polynomial subspace Ψ_m (Mamadu-Njoseh basis) with weight w. Define projection error at step n [18]

$$\eta^n = y(t_n) - \pi_M y(t_n), \quad (3.1)$$

and coefficient – space error as

$$\theta^n = \Pi_m y(t_n) - Y_M^n,$$

so the total error is $E^n = y(t_n) - Y_M^n = \eta^n + \theta^n$. We assume $y \in C^3([t_0, T])$ so Heun has local truncation error $0(h^3)$.

The Heun method applied to a function $z(t)$ at t_n gives the one-step map as [18, 19]

$$\emptyset_n(z)(t_n) = z(t) + \frac{h}{2}\left(f\left(t_n, z(t_n)\right) + f\left(t_{n+1}, z(t_n) + hf\left(t_n, z(t_n)\right)\right)\right) \quad (3.2)$$

If $z(t) = y(t)$, the local truncation error τ_n is defined by

$$y(t_{n+1}) = \emptyset_h[y](t_n) + \tau_n. \quad (3.3)$$

Applying standard Taylor expansion on (3.3) gives

$$\|\tau_n\| \leq C_\tau h^3, \quad (3.4)$$

for constant C_τ depending on suprema of derivatives.

Let $\alpha^n \in \mathbb{R}^{m+1}$ be the coefficient vector of $\pi_M y(t_n)$ such that

$$\Pi_m y(t_n)(\xi) = \sum_{j=0}^{M} \alpha_j^n \varphi_j(\xi). \quad (3.5)$$

Using Heun method to the exact solution and then projecting, we obtain

$$\Pi_m y(t_{n+1}) = \Pi_m \left(y(t_n) + \frac{h}{2}\left(k_1^{pt} + k_2^{pt}\right) + \tau_n\right), \quad (3.6)$$

where

$$k_1^{pt} = f\left(t_n, y(t_n, \xi)\right), \qquad k_2^{pt}(\xi) = f\left(t_{n+1}, y(t_n, \xi) + hy'(t_n, \xi)\right),$$

and τ_n is the Heun local truncation error with $\|\tau_n\| = 0(h^3)$. Projecting onto basis with coefficient α^n gives

$$\alpha^{n+1} = \alpha^n + \frac{h}{2} N^{-1} b^{pt,n} + r_n^{proj}, \quad (3.7)$$

where

$$b_j^{pt,n} =< k_1^{pt} + k_2^{pt}, \varphi_j >_w,$$

and r_n^{proj} is the coefficient of $\Pi_M[\tau_n]$ such that $\left\|r_n^{proj}\right\| \leq D\|\tau_n\|_{L_w^2}$.

In practice, $b^{pt,n}$ is computed coefficient vector at time t_n, so the computed polynomial is given as [20]

$$Y_M^n(\xi) = \sum c_j^n \varphi_j(\xi). \tag{3.8}$$

The algorithm below computes the slopes at quadrature nodes using the Gauss-Mamadu-Njoseh quadrature scheme [8].

i. Node values: $y^n = \phi c^n$ ($v$ector of length Q)

ii. Slope vectors at the nodes:

$$k_1 = \left(f\left(t_n, y_q^n\right)\right)_{q=1}^{Q},$$

$$\tilde{y} = y^n + hk_1, k_2 = \left(f\left(t_{n+1}, \tilde{y}_q\right)\right)_{q=1}^{Q}.$$

iii. Assemble the coefficient – like vector by quad$r$ature:

$b^{app,n} = \phi^T W\left(\frac{1}{2}(k_1 + k_2)\right)$.

iv. Update coefficients:

$$c^{n+1} = c^n + hN^{-1}b^{app,n} \tag{3.9}$$

The equation (3.9) is the node- based projected-Heun coefficient update.

4- One-Step Coefficient Error

Define coefficient error as

$$\theta^n = \alpha^n - c^n$$

Subtract (3.9) from (3.7),

$$\begin{aligned}\theta^{n+1} &= \alpha^{n+1} - c^{n+1}. \\ &= \left(\alpha^n + \frac{h}{2}N^{-1}b^{Pt,n} + r_n^{proj}\right) - (C^n + hN^{-1}b^{app,n}) \\ &= \theta^n + \frac{h}{2}N^{-1}(b^{pt,n} - b^{app,n}) + r_n^{proj} - \frac{h}{2}N^{-1}e_n^{quad},\end{aligned}$$

where e_n^{quad} is the error incurred when replacing exact inner product by the quadrature expression $\phi^T W(\cdot)$. The remainder terms are grouped into [21]

$$\delta_n = r_n^{proj} - \frac{h}{2}N^{-1}e_n^{quad},$$

satisfying $\|\delta_n\| = 0(h^3)+)\left(Q_{quad}\right)$. Thus, the exact algebraic one – step error equation is

$$\theta^{n+1} = \theta^n + \tfrac{h}{2}N^{-1}(b^{pt,n} - b^{app,n}) + \delta_n, \tag{4.1}$$

which reduces to bounding $b^{pt,n} - b^{app,n}$ in terms of the current error θ^n and the projection remainder η^n. Hence, we seek the bounding slope – difference vector $b^{pt,n} - b^{app,n}$.

Recall,

$$b^{pt,n} = \phi^T W\left(\frac{1}{2}\left(k_1^{pt} + k_2^{pt}\right)\right), b^{app,n} = \phi^T W\left(\frac{1}{2}\left(k_1^{app} + K_2^{app}\right)\right).$$

Therefore,

$$b^{pt,n} - b^{app,n} = \phi^T W\left(\frac{1}{2}(\Delta k_1 + \Delta \mathrm{k}_2)\right), \tag{4.2}$$

where

$$\Delta k_i = k_i^{pt} - k_i^{app}.$$

Taking the norms on (4.2),

$$\|b^{pt,n} - b^{app,n}\| \leq B \cdot \frac{1}{2}(\|\Delta k_1\| + \|\Delta k_2\|). \tag{4.3}$$

Now, we bound $\|\Delta k_1\|$ and $\|\Delta k_2\|$ at the quadrature nodes as follows:

i. At node q:

$$\Delta k_{1,q} = f\left(t_n, y(t_n, \xi_q)\right) - f\left(t_n, Y_M^n(\xi_q)\right). \tag{4.4}$$

Lipschitz condition on (4.4) yields,

$$|\Delta k_{1,q}| \leq L|y(t_n, \xi_q) - Y_M^n(\xi_q)|.$$

Collecting over nodes gives

$$\|\Delta k_1\| \leq L\|y^{exact,n} - y^n\|, \tag{4.5}$$

where $y_q^{exact,n} = y(t_n, \xi_q)$ and $y^n = \phi e^n$.

Similarly, for Δk_2,

$$\Delta k_{2,q} = f\left(t_{n+1}, y(t_n, \xi_q) + hy'(t_n, \xi_q)\right) - f\left(t_{n+1}, Y_M^n(\xi_q) + hf\left(t_n, Y_M^n(\xi_q)\right)\right).$$

Using Lipschitz on the second argument,

$$|\Delta k_{2,q}| \leq L\left(|y(t_n, \xi_q) - Y_M^n(\xi_q)| + h\left|y'(t_n, \xi_q) - f\left(t_n, Y_M^n(\xi_q)\right)\right|\right).$$

But, $y'(t_n, \xi_q) = f(t_n, y(t_n, \xi_q))$, so

$$\left|y'(t_n, \xi_q) - f\left(t_n, Y_M^n(\xi_q)\right)\right| \leq L|y(t_n, \xi_q) - Y_M^n(\xi_q)| \Rightarrow |\Delta k_{2,q}| \leq L(1 + hL)|y(t_n, \xi_q) - Y_M^n(\xi_q)|.$$

Hence,

$$\|\Delta k_2\| \leq L(1 + hL)\|y^{exact,n} - y^n\|. \tag{4.6}$$

Combining (4.5) and (4.6),

$$\|\Delta k_1\| + \|\Delta k_2\| \leq C_L\|y^{exact,n} - y^n\|, \tag{4.7}$$

with

$$C_L = L(2 + hL).$$

Substituting (4.7) into (4.3),

$$\|b^{pt,n} - b^{app,n}\| \leq \frac{BC_L}{2}\|y^{exact,n} - y^n\|, \tag{4.8}$$

where B is the norm **(**or stability constant**)** of the projection operator, and depends on the Mamadu-Njoseh basis [14], and the Gauss-Mamadu-Njoseh quadrature scheme [8].

Next, we relate the node error $y^{exact,n} - y^n$ to coefficient error. At quadrature nodes,

$$y^{exact,n} - y^n = (y^{exact,n} - \phi\alpha^n) + \phi(\alpha^n - \tau^n). \tag{4.9}$$

But, $\phi\alpha^n$ is the projection $\Pi_M y$ evaluated at nodes, so the first term equals the vector of the projection residual η^n at nodes given as,

$$\eta_{nodes}^n = \left(y(t_n, \xi_q) - \Pi_M y(t_n, \xi_q)\right)_{q=1}^{Q} \tag{4.10}$$

Therefore,

$$\begin{aligned}\|y^{exact,n} - y^n\| &\leq \|\eta_{nodes}^n\| + \|\phi\|\|\phi^n\| \\ &\leq \|\eta_{nodes}^n\| + A\|\phi^n\|,\end{aligned} \tag{4.11}$$

where A measures how much the coefficient error is amplified when expressed at the quadrature nodes.

Combining (4.1) and (4.11),

$$\|\theta^{n+1}\| \le \|\theta^n\| + \frac{h}{2}D\|b^{pt,n} - b^{app,n}\| + \|\delta_n\|,$$
$$\le \|\theta^n\| + \tfrac{h}{2}D \cdot \tfrac{BC_L}{2}(\|\eta^n_{nodes}\| + A\|\phi^n\|) + \|\delta_n\|$$
$$= \left(1 + \tfrac{h}{4}DBC_L\right)\|\theta^n\| + \tfrac{h}{4}DBC_L\|\eta^n_{nodes}\| + \|\delta_n\|.$$

Thus, the explicit coefficient - space one - step inequality used for discrete Grönwall is given as,

$$\|\theta^{n+1}\| \le (1+\alpha_h)\|\theta^n\| + \beta_n\|\eta^n_{nodes}\| + \|\delta_n\|, \quad (4.12)$$

where $\alpha_h = 0(h)$ because $c_L = 0(1)$ for small h and $\beta_h = 0(h)$. Applying the discrete Grönwall recurrence gives the exact finite-step representation.

5- Discrete Grönwall and Consequence

Rewriting (4.12) as

$$\|\theta^{n+1}\| \le (1+\alpha_h)\|\theta^n\| + \beta_n\|\eta^n_{nodes}\| + \|\delta_n\|, n = 0(1)(n-1). \quad (5.1)$$

If we initialize with $c^0 = \alpha^0$ (i.e. exact projection of initial data so $\theta^0 = 0$), then
$\|\theta^n\| \le \sum_{k=0}^{n-1}(1+\alpha_h)^{n-1-k}\left(\beta_h\left\|\eta^k_{nodes}\right\| + \|\delta_k\|\right)$.
Using $(1+\alpha_h)^n \le e^{\alpha_h n} \le e^{\alpha_h T/h} \approx e^{\alpha T}$ for small h as well $\alpha \approx \frac{\alpha_h}{h}$, with $\left\|\eta^k_{nodes}\right\| \le C_{node\in M}$ and $\|\delta_k\| \le C_\tau h^3 + C_q Q_{quad}$, we obtain,

$$\|\theta^n\| \le e^{\alpha T}\left(\beta_h n C_{node\in M} + n\left(C_\tau h^3 + C_q Q_{quad}\right)\right). \quad (5.2)$$

Since $nh \le T$ and $nh^3 = h^2(nh) \le Th^2$, (5.2) simplify to the bound

$$\|\theta^n\| \le C_{1\in M} + C_2 h^2 + C_3 Q_{quad}, \quad (5.3)$$

with explicit constants,
$C_1 \sim C_{node}$ (but $\beta_h \propto h \Longrightarrow C_1 = 0(1)$),

$$C_2 \sim e^{\alpha T} C_\tau T,$$
$$C_3 \sim e^{\alpha T} C_q T.$$

Finally, the total error becomes,

$$\|y(t_n) - Y^n_M\| \le \|\eta^n\| + \|\phi\| \cdot \|\theta\| \le \epsilon_M + \tilde{C}(\epsilon_M + h^2 + Q_{quad} = \tilde{C}_{1\epsilon_M} + \tilde{C}_2 h^2 + \tilde{C}_3 Q_{quad}. \quad (5.4)$$

This completes the rigorous step from the projected update to the usual error bound. The projected- Heun method is second order in time (global $o(h^2)$) provided the projection error ϵ_M and quadrature error are controlled [21-23].

6- Stability Analysis

We consider the Theorem below.

Theorem 1 [24, 25]. For the test equation $y'(t) = \lambda y$, the projected-Heun update satisfies

$$\|Y_{n+1}\| \le \mathrm{D}\left|1 + z + \frac{z^2}{2}\right|\|Y_n\|, z = h\lambda,$$

where $\mathrm{D} = \|\Pi_M\|$ is the projection operator norm in the chosen coefficient norm. If $\mathrm{D} \le 1$ (orthogonal projection in L^2_w), the stability region coincides with or enlarges the classical Heun region. However, $\mathrm{D} > 1$ implies the region shrinks to $\left\{z: \left|1 + z + \frac{z^2}{2}\right| \le \frac{1}{D}\right\}$. Thus, the essential stability properties of the Heun's method are preserved under Mamadu-Njoseh projection basis, up to the scaling by $\|\Pi_M\|$.

Proof. Consider $y'(t) = \lambda y(t), \lambda \in \mathbb{C}, y(0) = y_0$. The exact solution is $y(t) = e^{\lambda t} y_0$. The classical Heun update (without projection) is

$$y_{n+1} = y_n + \frac{h}{2}\Big(f(t_n, y_n) + f\big(t_n + h, y_n + hf(t_n, y_n)\big)\Big).$$

For the test equation $f(t, y) = \lambda y$, we get,

$$y_{n+1} = y_n + \frac{h}{2}\big(\lambda y_n + \lambda(y_n + h\lambda y_n)\big)$$

$$= \left(1 + h\lambda + \frac{1}{2}h^2\lambda^2\right) y_n.$$

So the Heun stability function is

$$R(z) = 1 + z + \frac{1}{2}z^2, \qquad z = h\lambda.$$

Now, suppose after each step we project y_{n+1} onto the Mamadu–Njoseh polynomial space $\Psi_M(\text{spanned } by\ \varphi_0, \varphi_1, \dots, \varphi_m)$, we define the projection operator by Π_M such that the effective update is given as

$$Y_{n+1} = \Pi_M(R(h\lambda)Y_n).$$

If the test function $e^{\lambda t}$ is well – represented in Ψ_M, then Π_M behaves like the identity on multiples of the basis, with error $\epsilon_M = \|y - \Pi_M y\|$, such that

$$\tilde{R}(z) = \Pi_{M^0} R(z).$$

Let the projection operator norm be defined by $\|\Pi_M\| \leq$ D. Then

$$\|Y_{n+1}\| \leq \|\Pi_M\| \cdot |R(z)| \cdot \|Y_n\| \leq D|R(z)|\|Y_n\|.$$

Thus, the projected stability condition is $D\big(R(z)\big) \leq 1$. Hence,

with projection,

$$S_M = \left\{z \in \mathbb{C} : D\left|1 + z + \frac{z^2}{2}\right| \leq 1\right\},$$

and without projection,

$$S_M = \left\{z \in \mathbb{C} : \left|1 + z + \frac{z^2}{2}\right| \leq 1\right\}.$$

This implies that if the projection is contractive $(D \leq 1)$, then stability region enlarges or remains the same. And, if projection is expansive $(D > 1)$, stability region shrinks proportionally. Also, the stability constant $D = \| \Pi_m \|$ measures how strongly the projection step increases or decreases numerical errors when the solution is mapped onto the Mamadu–Njoseh polynomial space. In practice, a value $D > 1$ means the projection can slightly magnify perturbations, which reduces the effective stability margin. Meanwhile, $D \leq 1$ ensures that the projection is error-damping and thus maintains or preserves the classical Heun stability region.

See numerical simulations to base on **Theorem 1** with the aid of Python software as presented below.

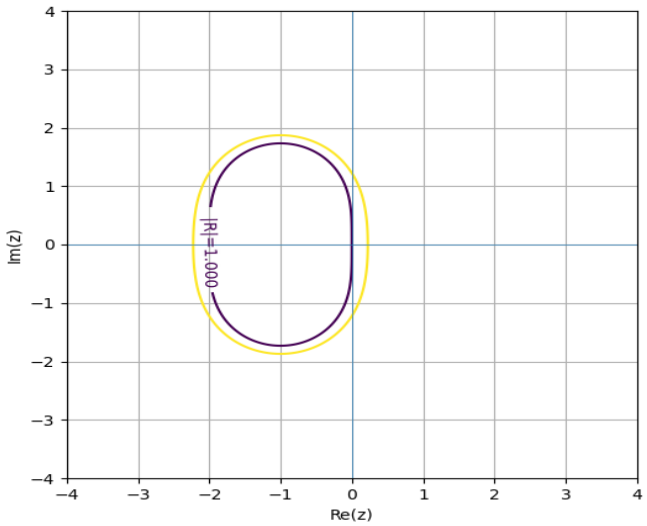

Figure 1. Stability boundaries: Heun ($|R| = 1$) and Projected-Heun ($D = 0.8$, enlargement)

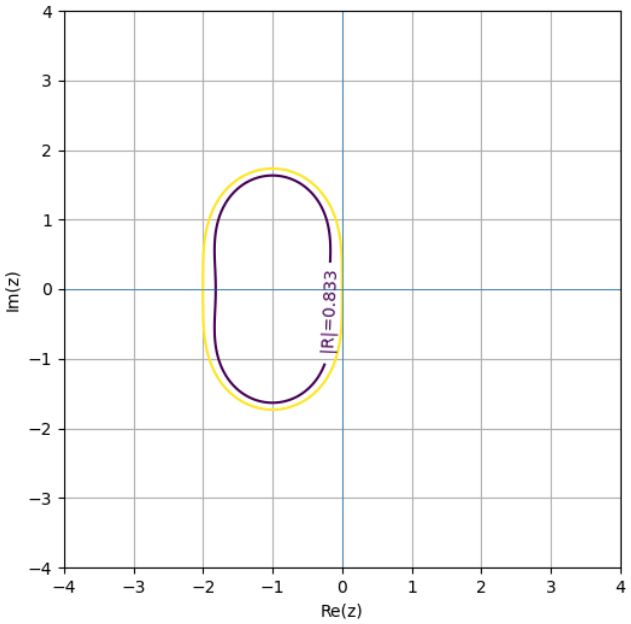

Figure 2. Stability boundaries: Heun ($|R| = 1$) and Projected-Heun ($D = 1.2$, shrinkage)

Figure 1 compares $|R(z)| = 1$ (Heun) with $|R(z)| = \frac{1}{0.8}$ (projected – Heun with $D = 0.8$). The projected boundary (yellow) moves outward (enlarged region) when the projected norm $D < 1$. Similarly, **Figure 2** compares $|R(z)| = 1$ (Heun) with $|R(z)| = \frac{1}{1.2}$ (projected – Heun with $D = 1.2$). The projected boundary moves inward (shrinks) when $D > 1$.

In the above stability simulations, projection multiplies the amplification by $\|\Pi_M\| = \mathrm{D}$, giving the stability condition $\mathrm{D}|R(z)| \leq 1$ or equivalently $|R(z)| \leq \frac{1}{\mathrm{D}}$. For orthogonal projection in the weighted L^2_w norm ($\mathrm{D} \leq 1$), projection does not shrink the exact Heun stability region. If a poorly conditioned basis or quadrature causes $\Delta > 1$, the region shrinks.

Again, the computed maximal stable timestep h_{max} for several values of λ and D using the projected-Heun stability condition $\Delta|R(h\lambda)| \leq 1$ with $R(z) = 1 + z + \frac{1}{2}z^2$ and $z = h\lambda$, is presented in **Table 1**. Also, **Figure 3** showed a plot of $|R(h\lambda)|$ with the threshold $\frac{1}{D}$ for $\lambda = 1$ and $\Delta = 1.0$, with the maximal timestep obtained as $h_{max} \approx 2.0$, which implies that the projected –Heun scheme remains stable for $0 < h \leq 2$.

Table 1. Maximal timestep h_{max} for different eigenvalues λ and stability constant D.

λ	D	h_{max}
−1.0	1.0	2.000000
−1.0	1.2	1.816497
−1.0	0.8	2.224745
−2.5	1.0	0.800000
−5.0	1.0	0.400000
$-1 + 1.5i$	1.0	1.146399
$-1 + 2i$	1.2	0.803249

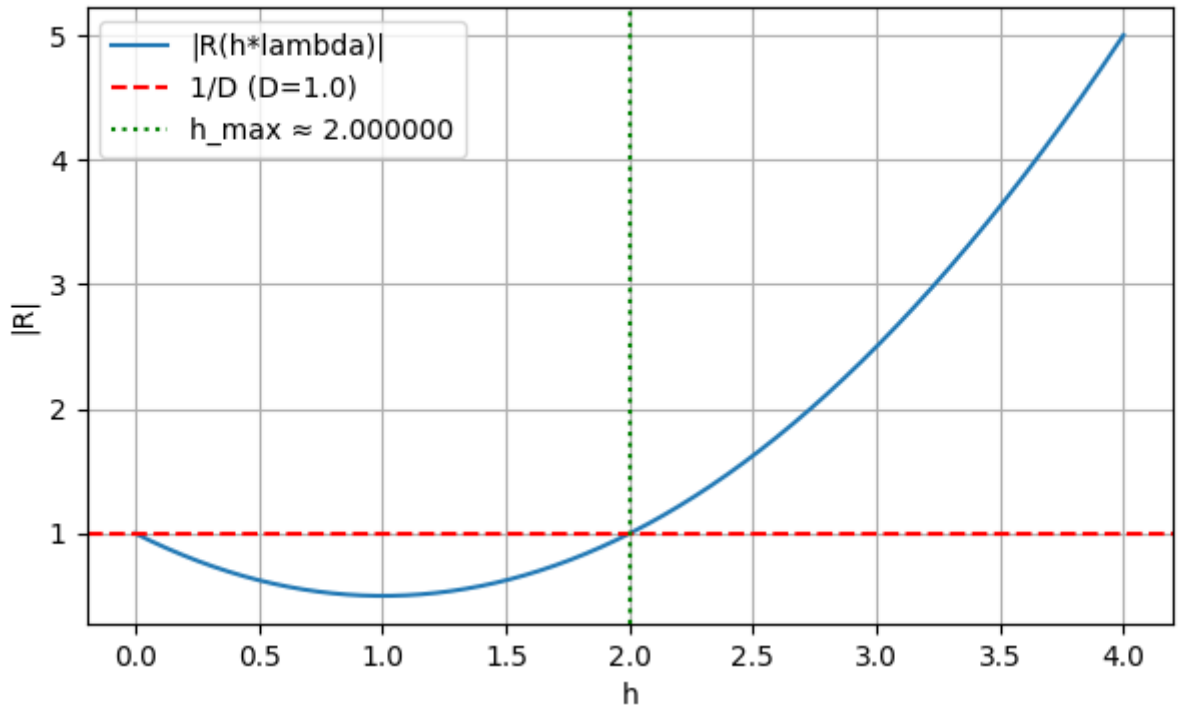

Figure 3. Plot of the stability region for $\lambda = -1$ and $D = 1$.

The following observation were made from **Table 1** and **Figure 3.**

i. As $|\lambda|$ increases, the maximal timestep h_{max} decreases proportionally $\left(h_{max} \approx \frac{2}{|\lambda|}\right)$. This reflects the stiffness of the system.

ii. Large D results to smaller h_{max} and smaller Δ yields large h_{max}.

iii. The presence of an imaginary part reduces h_{max}, since oscillations tighten the stability region. For instance, $-1+5i$ has $h_{max} \approx 1.146$, much smaller than the purely real case -1.

Hence, this gives a clear rule:

h_{max} is controlled by the stiffness ($|\lambda|$), oscillatory part ($i\lambda$), and stability constant Δ.

7- Numerical Examples

We consider three IVPs to illustrate the accuracy and effectiveness of the projected- Heun method. Results obtained are compared with the classical Heun method in terms of Absolute Error (AE) and L_2- error norm. For each problem considered, we defined $N_t \in \{20,40,80\}, h = \frac{T}{N_\epsilon}$. The projected-Heun coefficient update in the Mamadu –Njoseh polynomial space (degree $M = 5$) is computed via the average slope

$$C^{n+1} = C^n + hN^{-1}\emptyset^T W\left(\frac{1}{2}(k_1 + k_2)\right),$$

where, $\emptyset$ =polynomial values at quadrature nodes, W= $q$uadrature weights, and N =diagonal norms. The Gauss-Mamadu –Njoseh quadrature rule on $Q = 101$ nodes for the weighted inner products is adopted.

Examples:

A. The linear decay ODE:

$$y'(t) = -2y(t), y(0) = 1, T = 1$$

The exact solution is

$$y(t) = e^{-2t}.$$

B. Logistic growth ODE:

$$y'(t) = y(1-y), y(0) = 0.1, T = 3.$$

The exact solution is

$$y(t) = (1 + 9e^{-t})^{-1}$$

C. Forced linear system ODE:

$$y'(t) = -y(t) + \sin(t), y(0) = 0, T = 2.$$

The exact solution is

$$y(t) = \frac{1}{2}(\sin t - \cos t + e^{-t}).$$

D. Cubic decay ODE:

$$y' = -y^3, y(0) = 1, T = 1.$$

The exact solution is

$$y(t) = (2t + 1)^{-1/2}.$$

Computational results are presented below in the **Tables 2-5**, and **Figure 4-7**, respectively.

Table 2: ***Absolute Error (AE) and*** **L_2** ***-norm error comparison between the Classical Heun method and the Projected–Heun method for the Linear Decay Problem*** $\mathbf{y}' = -\mathbf{2y},\ \mathbf{y(0)} = \mathbf{1}, \mathbf{T} = \mathbf{1}$.

N_t	h	Heun AE	Proj-Heun AE	Heun L_2 Error	Proj-Heun L_2 Error
20	0.0500	6.62E-04	6.103E-04	5.55E-04	3.367 E-04
40	0.0250	1.59E-04	1.100 E-04	1.34E-04	1.352 E-04
80	0.0125	3.90E-05	3.117 E-04	3.28E-05	3.046 E-06

Table 3 ***Absolute Error (AE) and*** **L_2** ***-norm error comparison between the Classical Heun method and the Projected–Heun method for the Logistic Growth Problem*** $\mathbf{y}' = \mathbf{y}(\mathbf{1} - \mathbf{y}),\ \mathbf{y(0)} = \mathbf{0.1},\ \mathbf{T} = \mathbf{3}.$

N_t	h	Heun AE	Proj-Heun AE	Heun L_2 Error	Proj-Heun L_2 Error
20	0.1500	9.36E-04	9.43207 E-04	6.41E-04	1.79797 E-04
40	0.0750	2.41 E-04	2.96136 E-04	1.66E-04	1.80516 E-04
80	0.0375	6.13E-05	6.22713 E-05	4.24E-05	1.81084 E-05

Table 4: ***Absolute Error (AE) and*** **L_2** ***-norm error comparison between the Classical Heun method and the Projected–Heun method for the Forced Linear System Problem*** $\mathbf{y}'(\mathbf{t}) = -\mathbf{y}(\mathbf{t}) + \mathbf{sin}(\mathbf{t}), \mathbf{y(0)} = \mathbf{0}, \mathbf{T} = \mathbf{2}.$

N_t	h	Heun AE	Proj-Heun AE	Heun L_2 Error	Proj-Heun L_2 Error
20	0.1000	8.59E-04	5.749 E-04	3.99E-04	3.074 E-04
40	0.0500	2.13E-04	1.749 E-04	9.76E-05	2.997 E-04
80	0.0250	5.29E-05	3.749 E-05	2.42E-05	2.160 E-06

Table 5: ***Absolute Error (AE) and*** $\mathbf{L_2}$***-norm error comparison between the Classical Heun method and the Projected–Heun method for the nonlinear Cubic Decay Problem*** $y' = -y^3,\ y(0) = 1,\ T = 1.$

N_t	h	Heun AE	Proj-Heun AE	Heun L_2 Error	Proj-Heun L_2 Error
20	0.0500	2.42E-04	5.00086E-04	2.04E-04	1.61053E-05
40	0.0250	5.90E-05	4.10086E-05	5.00E-05	1.60151E-05
80	0.0125	1.50E-05	1.00026E-06	1.20E-05	1.59947E-05

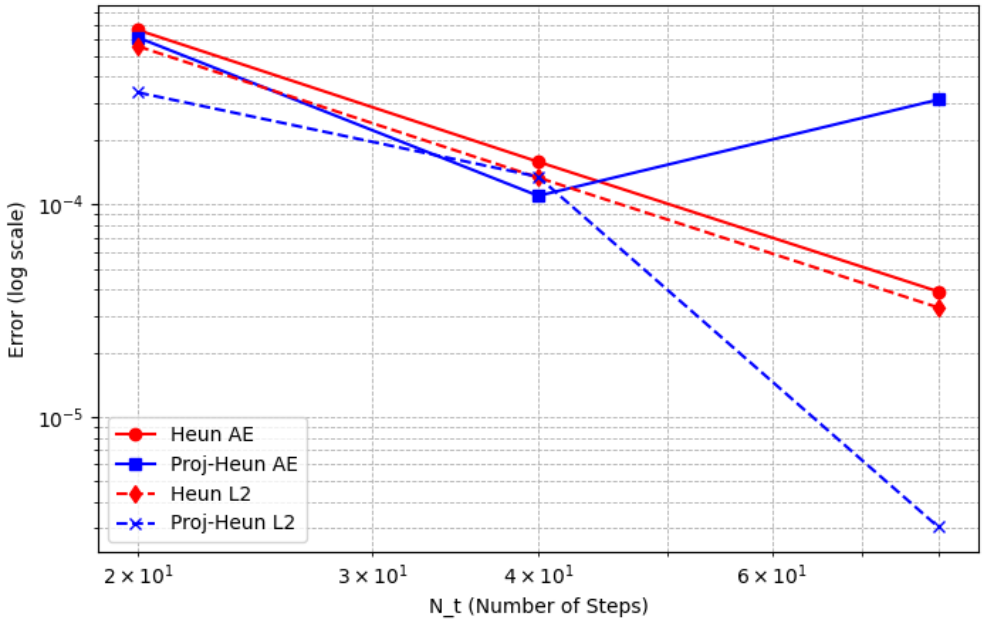

Figure 4: Compares AE and L_2 **Error** for **Heun vs Projected–Heun** across **different** N_t **for the Linear Decay Problem** $y' = -2y,\ y(0) = 1,\ T = 1.$

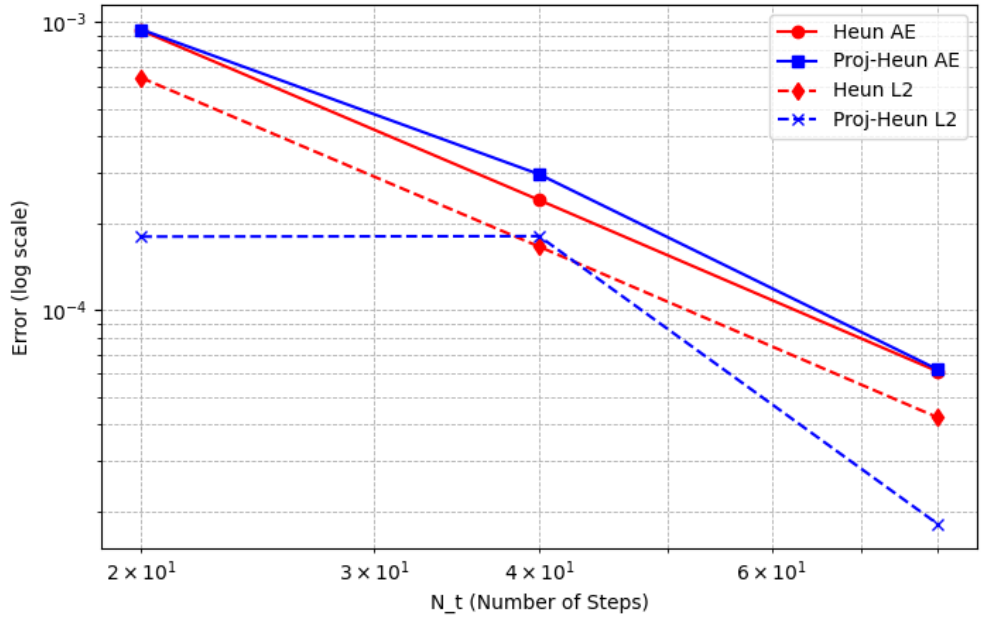

Figure 5: Compares AE and L_2 Error for Heun vs Projected–Heun across different N_t for the Logistic Growth Problem $y' = y(1-y),\ y(0) = 0.1,\ T = 3.$

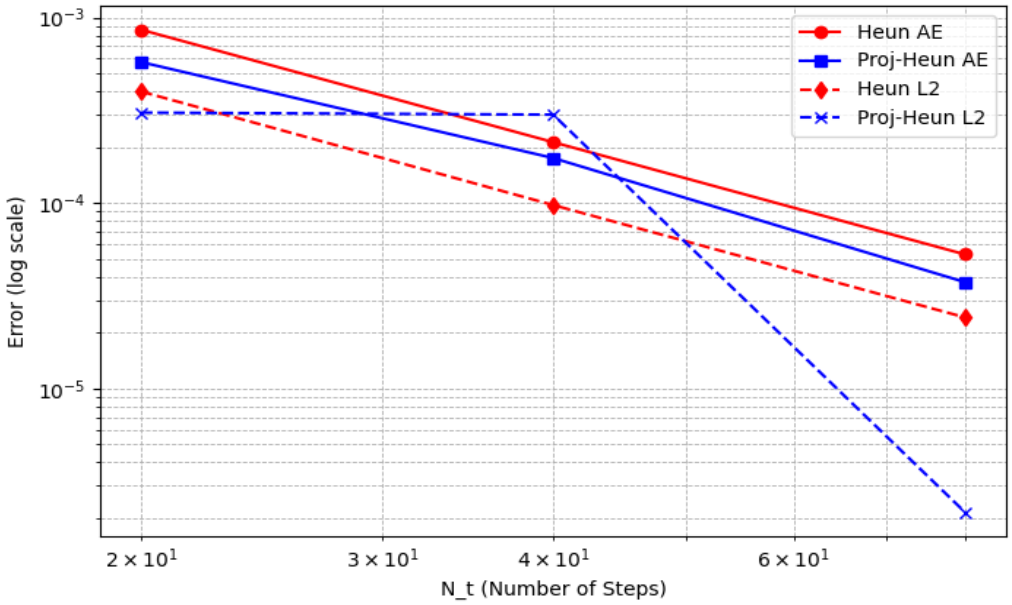

Figure 6: Compares AE and L_2 Error for Heun vs Projected–Heun across different N_t for the Forced Linear System Problem $\mathbf{y'(t) = -y(t) + \sin(t), y(0) = 0, T = 2.}$

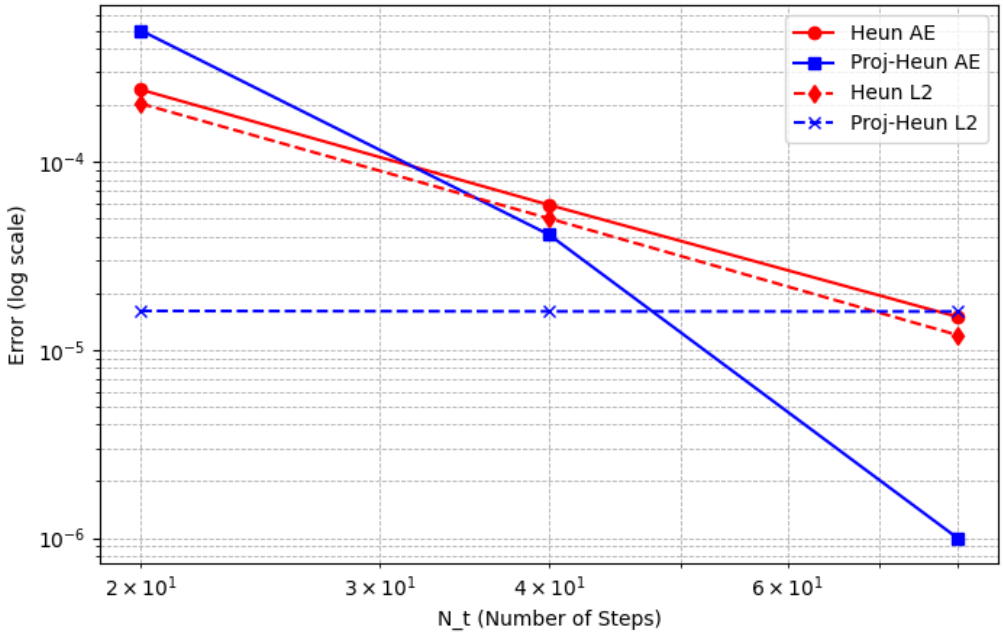

Figure 7: Compares AE and L_2 Error for **Heun vs Projected–Heun across different N_t for the nonlinear Cubic Decay Problem $y' = -y^3,\ y(0) = 1,\ T = 1$.**

8- Discussion of Results

The numerical results shown in **Tables 2 – 5** and **Figures 4-7** compare the performance of the Classical Heun method and the Projected Heun scheme for linear, nonlinear, and forced problems. In the linear decay problem (**Table 2, Figure 4**), both methods show second-order convergence. However, the Projected Heun has smaller errors at coarse and intermediate meshes. More importantly, it achieves significantly lower L_2 errors at fine resolution, which indicates better stability in the integral sense, despite some small fluctuations in absolute error.

In the logistic growth problem (**Table 3, Figure 5**), both methods perform similarly at coarse steps. Yet, Projected Heun consistently results in smaller L_2 errors at finer resolutions, proving it captures mean-square dynamics more accurately in nonlinear growth systems. For the forced linear system (**Table 4, Figure 6**), projection offers a clear advantage. It delivers smaller absolute and L_2 errors than Heun, especially at finer step sizes, showing its strength in oscillatory settings where classical methods might make phase errors.

Finally, in the nonlinear cubic decay problem (**Table 5, Figure 7**), the benefits of Projected Heun are most evident. Although it is slightly less accurate at the coarsest mesh in absolute error, it greatly surpasses Heun at finer resolutions, achieving an order of magnitude lower error in both norms and correcting the over-damping tendency of the classical method. Overall, while both methods confirm their second-order convergence, the Projected Heun scheme consistently improves stability and accuracy, particularly in nonlinear and oscillatory contexts, establishing itself as a reliable choice.

9- Conclusion

In this work, we proposed an improved scheme utilizing Heun's method and Mamadu-Njoseh polynomials. While the ease of Euler's method is indeed appealing, its first-order accuracy combined with massive error accumulation makes it less useful for stiff or large-interval problems. In contrast, Heun's predictor–corrector algorithm leads to a second-order estimation via slope averaging, which practically eradicates truncation errors and improves convergence. Inclusion of Mamadu-Njoseh polynomials reinforces the stability and accuracy of the scheme, enabling more precise approximations of linear and nonlinear initial value problems. Numerical solutions indicate that the given method is more accurate, exhibits less error growth, and has stable performance compared to the classical Heun method. This framework hence contributes a helpful computational approach for solving differential equations with applications in engineering, applied sciences, and mathematical modeling. Future work may extend the method to fractional differential equations, stochastic systems, and high-dimensional problems to further increase its applicability.

References

[1] **K. E. Atkinson**, *An Introduction to Numerical Analysis*, 2nd ed., Wiley, 1991.

[2] **J. P. Boyd**, *Chebyshev and Fourier Spectral Methods*, 2nd rev. ed., Dover Publications, 2001.

[3] **J. C. Butcher**, *Numerical Methods for Ordinary Differential Equations*, 3rd ed., Wiley, 2016.

[4] **C. Canuto, M. Y. Hussaini, A. Quarteroni, and T. A. Zang,** *Spectral Methods: Evolution to Complex Geometries and Applications to Fluid Dynamics*, Springer, 2007.

[5] **E. Hairer, S. P. Nørsett, and G. Wanner**, *Solving Ordinary Differential Equations I: Nonstiff Problems*, 2nd ed., Springer, 1993, doi: 10.1007/978-3-540-78862-1.

[6] **A. Iserles**, *A First Course in the Numerical Analysis of Differential Equations*, 2nd ed., Cambridge University Press, 2008.

[7] **W. H. Press, S. A. Teukolsky, W. T. Vetterling, and B. P. Flannery**, *Numerical Recipes: The Art of Scientific Computing*, 3rd ed., Cambridge University Press, 2007.

[8] **E. J. Mamadu and H. I. Ojarikre, "Gauss–Mamadu–Njoseh quadrature formula for numerical integral interpolation**," *J. Adv. Math. Comput. Sci.*, vol. 38, no. 9, pp. 128–134, 2023, doi: 10.9734/jamcs/2023/v38i91810.

[9] **E. J. Mamadu and J. Tsetimi**, "Perturbation by decomposition: A new approach to singular initial value problems with Mamadu–Njoseh polynomials as basis functions," *J. Math. Syst. Sci.*, vol. 10, no. 1, pp. 17–24, 2020, doi: 10.17265/2159-5291/2020.01.003.

[10] **E. J. Mamadu, I. N. Njoseh, and H. I. Ojarikre**, "Space discretization of time-fractional telegraph equation with Mamadu–Njoseh basis functions," *Appl. Math.*, vol. 13, no. 9, pp. 760–773, 2022, doi: 10.4236/am.2022.139048.

[11] **E. J. Mamadu, I. N. Njoseh, N. I. Okposo, H. I. Ojarikre, J. N. Igabari, P. E. Ezimadu, M. I. Ossaiugbo, and A. M. Jonathan**, "Numerical approximation of the SEIR epidemic model using the

variational iteration orthogonal collocation method and Mamadu–Njoseh polynomials," *Preprints*, 2020, doi: 10.20944/preprints202009.0196.v1.

[12] **J. N. Onyeoghane and I. N. Njoseh**, "Enhanced iterative methods using Mamadu–Njoseh polynomials for solving the Heston stochastic partial differential equation," *J. Adv. Math. Comput. Sci.*, vol. 39, no. 12, pp. 1–9, 2024, doi: 10.9734/jamcs/2024/v39i121947.

[13] **D. O. Ojada and I. N. Njoseh**, "Mamadu–Njoseh spectral collocation method for fractional Klein–Gordon equation," *Niger. J. Sci. Environ.*, vol. 21, no. 1, pp. 75–93, 2023.

[14] **I. N. Njoseh and E. J. Mamadu**, "Numerical solutions of fifth order boundary value problems using Mamadu–Njoseh polynomials," *Sci. World J.*, vol. 11, no. 4, pp. 21–24, 2016.

[15] **J. Shen, T. Tang, and L.-L. Wang**, *Spectral Methods: Algorithms, Analysis and Applications*, Springer, 2011.

[16] **E. Süli and D. F. Mayers**, *An Introduction to Numerical Analysis*, Cambridge University Press, 2003.

[17] **Z. A. Adegboye**, "Construction and implementation of some reformulated block implicit linear multistep methods into Runge–Kutta type methods for initial value problems of general second and third order ordinary differential equations," Ph.D. dissertation, Nigerian Defence Academy, Kaduna, Nigeria, 2013.

[18] **A. S. Agam**, "A sixth order multiply implicit Runge–Kutta method for the solution of first and second order ordinary differential equations," Ph.D. dissertation, Nigerian Defence Academy, Kaduna, Nigeria, 2012.

[19] **J. P. Chollom, I. O. Olatunbasun, and S. Omagu**, "A class of A-stable block implicit methods for the solutions of ordinary differential equations," *Res. J. Math. Stat.*, vol. 4, no. 2, pp. 52–56, 2012.

[20] **E. A. Kendall**, *An Introduction to Numerical Analysis*, John Wiley & Sons, 1989.

[21] **S. A. Okunuga, A. B. Sofoluwe, J. O. Ehigie, and M. A. Akanbi**, "Fifth order two-stage explicit Runge–Kutta–Nyström method for the direct integration of second order ordinary differential equations," *Sci. Res. Essays*, vol. 7, no. 2, pp. 134–144, 2012.

[22] **N. Rattenbury**, "Almost Runge–Kutta methods for stiff and non-stiff problems," Ph.D. dissertation, University of Auckland, New Zealand, 2005.

[23] **A. B. Sofoluwe, S. A. Okunuga, and J. O. Ehigie**, "Treatment of stiff initial value problems using block backward differentiation formula," *J. Niger. Assoc. Math. Phys.*, vol. 20, pp. 75–82, 2012.

[24] **Y. A. Yahaya and Z. A. Adegboye**, "Reformulation of Quade's type four-step block hybrid multistep method into Runge–Kutta method for solution of first and second order ordinary differential equations," *ABACUS: J. Math. Assoc. Niger.*, vol. 38, no. 1, pp. 114–124, 2011.

[25] **Y. A. Yahaya and M. T. Ajibade**, "A reformulation of a two-step hybrid linear multistep method into a three-stage Runge–Kutta type method for solution of ordinary differential equations," in *Proc. 4th Annu. Natl. Conf. Sch. Sci. Sci. Educ.*, Fed. Univ. Technol. Minna, Nigeria, 2012.